Journal of Alloys and Compounds 524 (2012) 69–72

Contents lists available at SciVerse ScienceDirect

Journal of Alloys and Compounds

journal homepage: www.elsevier.com/locate/jallcom

The contributions of intrinsic damping and two magnon scattering on the ferromagnetic resonance linewidth in $[Fe_{65}Co_{35}/SiO_2]_n$ multilayer films

Bailin Liu[a,b], Yi Yang[a,*], Dongming Tang[a], Baoshan Zhang[a], Mu Lu[a], Huaixian Lu[a]

[a] School of Electronic Science and Engineering, Nanjing University, Nanjing, Jiangsu 210093, China
[b] Southwest Technology and Engineering Research Institute, Chongqing 400039, China

ARTICLE INFO

Article history:
Received 26 September 2011
Received in revised form 2 February 2012
Accepted 7 February 2012
Available online 16 February 2012

Keywords:
FMR
Damping mechanisms
Extrinsic linewidth
Intrinsic linewidth
Two magnon scattering
Multilayer films

ABSTRACT

In order to investigate microwave damping mechanisms of ferromagnetic films with a structure of [ferromagnetic (FM)/non-magnetic insulator (NMI)]$_n$, a serial of $[Fe_{65}Co_{35}/SiO_2]_n$ multilayer films was prepared by a magnetron sputtering method on the glass substrate. As-prepared films show excellent soft magnetic properties with tiny coercivities along the easy and hard axis respectively, and remarkable in-plane unixial anisotropies were observed too. The microwave properties were characterized by the ferromagnetic resonance (FMR) and a broadband permeameter. The corresponding theoretical fitting was conducted based on the Landau–Lifshitz–Gilbert (LLG) and two magnon scattering (TMS) theory. Fitting results show the TMS linewidth has a value of 36 times bigger than Landau–Lifshitz intrinsic linewidth, which gives a quantitative and explicit physical picture of microwave damping mechanisms in $[Fe_{65}Co_{35}/SiO_2]_n$ multilayer films and may be important for the understanding of damping in [FM/NMI]$_n$ multilayer films.

1. Introduction

In recent years, there has been an extensive research on microwave properties of ferromagnetic thin films to satisfy many requirements of advances in the wireless technology such as WiFi networks, real-time mobile communication in GHz frequency band [1]. Ferromagnetic thin films attract more interest of researchers because of their combined properties of the high saturation magnetization, controllable in-plane anisotropy field, high permeability in GHz range, high electrical resistivity for reducing the eddy current loss and other interesting physical phenomena [2,3]. Compared to usual single-layer nano-granular films whose magnetic grains are separated in the insulating amorphous phase, multilayer films with a microstructure of [magnetic metal/insulator]$_n$ could be more effective and convenient to obtain higher resistivity for high frequency applications meanwhile maintaining their soft magnetic properties [4]. For these purposes, it is important to get a better understanding of the damping mechanism of ferromagnetic multilayer films.

Up to now, there are lots of published theoretical and experimental results on the microwave damping mechanism of magnetic materials [5–13]. More attentions have been paid to the damping in the single-layer nano-granular magnetic film [10,11], magnetic alloy film [14] and the multilayer film with a structure of [ferromagnetic (FM)/non-magnetic metal (NMM)]$_n$ [12,13]. However, the damping mechanism of multilayer films with the structure of [ferromagnetic (FM)/non-magnetic insulator (NMI)]$_n$ has been less considered recently. Obviously, the damping mechanism in [FM/NMI]$_n$ multilayer films is more complicated and will be more interesting for the understanding of the spin dynamics in ferromagnetic films. It will give a theoretical guidance to prepare all kinds of magnetic films for high-frequency microwave absorption applications.

In the present work, multilayer films of $[Fe_{65}Co_{35}/SiO_2]_n$ were prepared by the magnetron sputtering. Microwave properties of some typical samples were determined by the ferromagnetic resonance (FMR) and a broadband permeameter. Especially, we focus on damping origins of those multilayer films. The dependences of the FMR field H_{RES} and FMR linewidth ΔH_{RES} on the polar angle θ of the external field, measured from the FMR, have been successfully fitted based on the Landau–Lifshitz–Gilbert (LLG) equation and two-magnon scattering (TMS) theory. From fitting results, a quantitative relationship between the Landau–Lifshitz (L–L) intrinsic and TMS extrinsic damping has been obtained.

2. Experiments

A serial of $[Fe_{65}Co_{35}/SiO_2]_n$ multilayer films was prepared by a magnetron sputtering method on the glass substrates. Before sputtering, a 10 nm Ta buffer layer was first deposited on the substrate. Two separate targets, $Fe_{65}Co_{35}$ and SiO_2, were set to sputter alternately with the same power of 40 W. The thickness of all the

* Corresponding author. Tel.: +86 25 83593011; fax: +86 25 83593011.
E-mail address: malab@nju.edu.cn (Y. Yang).

0925-8388/$ – see front matter © 2012 Elsevier B.V. All rights reserved.
doi:10.1016/j.jallcom.2012.02.060

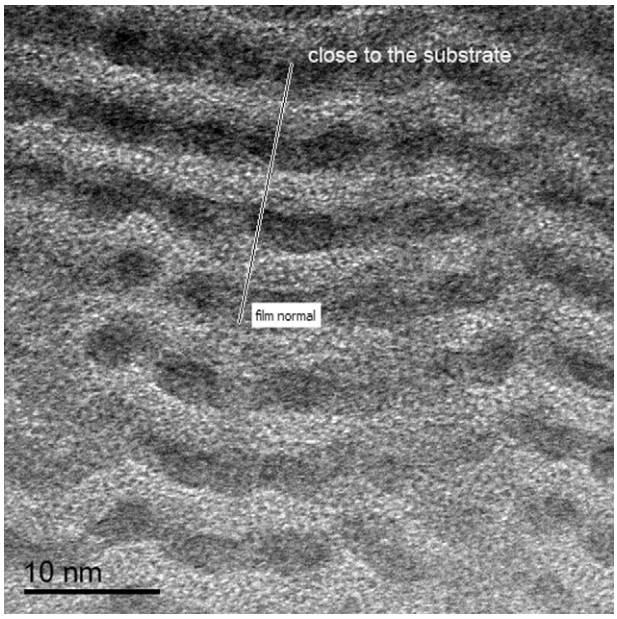

Fig. 1. The bright-field HRTEM images of the cross-section for the sample S1.

layers was controlled by the time of the substrate staying on each target. During sputtering, an in-plane external static magnetic field of about 150 mT was applied to induce a uniaxial magnetic anisotropy. The static magnetic properties were measured using a vibrating sample magnetometer (VSM). The microstructure of the films was determined by the high resolution transmission electronic microscopy (HRTEM). Microwave magnetic properties were characterized by the FMR measurement using a shorted waveguide at 9.78 GHz. The permeability spectra were measured by a broadband one-port microstrip permeameter in combination with the Agilent network analyzer from 200 MHz to 9 GHz [15]. All measurements were carried out at room temperature.

3. Results and discussions

Fig. 1 displays the bright-field HRTEM images of the cross-section for the sample named S1 with a structure of $[Fe_{65}Co_{35}/SiO_2]_{20}$. It can be seen that the sequential deposition of FeCo and SiO_2 layers produces a nanogranular multilayer structure appearing as most of FeCo planes isolated by amorphous SiO_2 layers. The thicknesses for FeCo and SiO_2 layers are respectively about 2.5 nm and 2.1 nm. This structure differs from conventional nanogranular magnetic films, and presents more magnetic inhomogeneities.

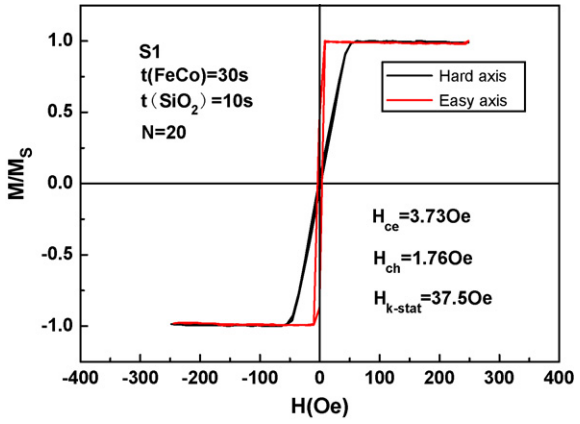

Fig. 2. The magnetization curves of the sample S1 measured by VSM with easy axis coercive force (H_{ce}) equal to 3.73 Oe, hard axis coercive force equal to 1.76 Oe, and static uniaxial anisotropy ($H_{k\text{-}stat}$) field equal to 37.5 Oe.

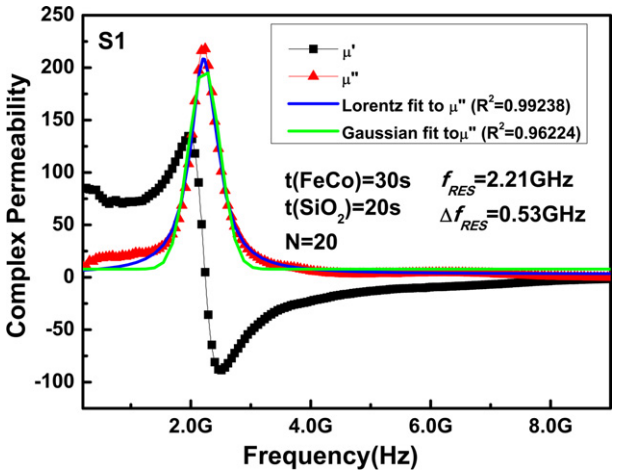

Fig. 3. The frequency-dependent permeability of sample S1 measured by a broadband one-port microstrip permeameter without an external field parallel to the easy axis. The inset in the right corner is the schematic of permeameter. The natural resonance frequency (f_{RES}) equal to 2.21 GHz, the resonance linewidth (Δf_{RES}) equal to 0.53 GHz.

Fig. 2 shows magnetization curves for the sample S1. The coercivities H_{ce} and H_{ch}, respectively along the easy and hard axis, are 3.73 Oe and 1.76 Oe. The static in-plane anisotropy field $H_{k\text{-}stat}$ is about 37.5 Oe, which is calculated by the integration of reduced magnetization between the easy axis and hard axis loops [16]. These soft magnetic properties can be attributed to the exchange interaction among magnetic grains in the same layer and the interlayer exchange coupling which exists between adjacent magnetic FeCo layers across the nonmagnetic SiO_2 interlayers. According to the assumption in Refs. [17,18], if thin enough, the SiO_2 interlayer will be not continuous but contain a lot of pinholes, through which the two FeCo films will be in contact. The magnetization in the adjacent FeCo layers will be forced to align parallel. Consequently, the local magneto-anisotropies of magnetic grains and the demagnetization effects will be averaged out over an increasing number of magnetic grains, such that an in-plane uniaxial anisotropy can be induced by an external field during the sputtering process. It should be mentioned that the presence of pin-hole will reduce the resistivity of films, but it is necessary for multilayer films and granular films to perform magnetic exchange interaction. They can still achieve higher resistivity than pure metal films.

In order to investigate microwave properties of the $[Fe_{65}Co_{35}/SiO_2]_n$ multilayer films, we observed the permeability spectra of the sample S1. Fig. 3 shows the frequency-dependent permeability of the sample S1, which was measured using a broadband one-port microstrip permeameter without an external field parallel to the easy axis of the sample. First, the permeability spectra have a legible resonance peak at 2.21 GHz with a full-width at half-maximum (FWHM) about 0.53 GHz, and this resonance is not in a relaxation type but a resonance type, which indicates that the spin precession along the easy axis in the film almost keeps in an uniform mode. Second, the regression parameter R^2 from the Lorentz fit is more close to 1 than that from the Gaussian fit. It is reasonable to say that the line shape of the permeability spectra is more likely a Lorentzian, which implies that the contribution to the damping linewidth mainly comes from the two-magnon scattering and intrinsic damping [19].

Fig. 4 shows the imaginary part of complex permeability of the sample S1 measured with different external fields. The external field H_b was applied along the easy axis and in the plane of the sample. Some parameters obtained from Fig. 4 are plotted in Fig. 5 for comparison, including the resonance frequency f_{RES} and the frequency linewidth Δf_{RES}. It can be seen that the resonance

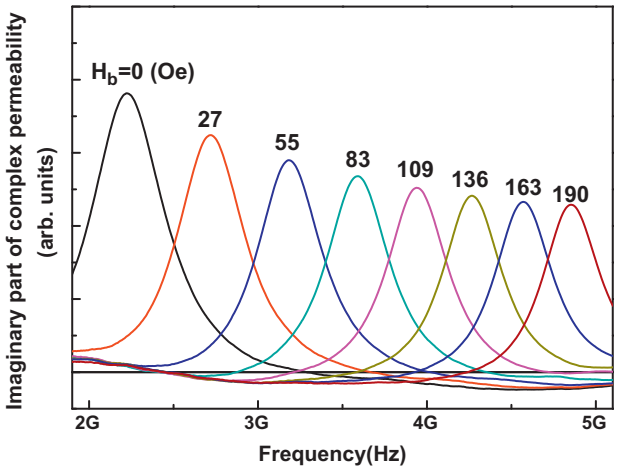

Fig. 4. The microwave permeability spectra of the sample S1 in different external fields H_b. The data listed above the curves are values of external fields parallel to the direction of the in-plane uniaxial anisotropy.

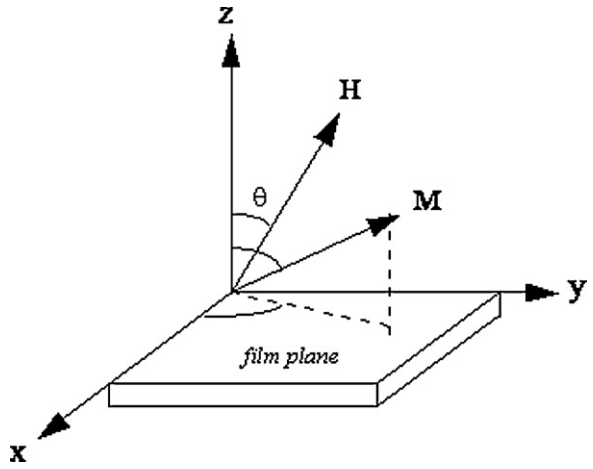

Fig. 6. The film plane and the field geometry for FMR analysis. The in-plane uniaxial anisotropy can lie in any direction for it is small enough compared with the external field.

frequency f_{RES} increases with the increased H_b. The dependence of f_{RES} on H_b is in correspondence with Kittel equation $f_{RES} = \gamma\sqrt{(H_k + H_b)(4\pi M_S + H_k + H_b)}$. Meanwhile, the Δf_{RES} decreases with the increased H_b. Here, the Δf_{RES} can be decomposed into intrinsic and extrinsic parts, that is to say, $\Delta f_{RES} = \Delta f_{INT} + \Delta f_{EXT}$ [20]. As reported in Ref. [21], the intrinsic damping originates from the spin-orbital coupling, and according to the LLG equation, the intrinsic linewidth Δf_{INT} will increase linearly with the increasing H_b [9]. Hence, the extrinsic linewidth Δf_{EXT} must decreases more sharply than Δf_{INT}. It implies that the extrinsic contribution may be larger than the intrinsic part to the damping linewidth. The decrease of Δf_{EXT} can be attributed to the influence of the external field on the magnetizations in the film. Generally, the inhomogeneities in ferromagnetic films, such as defects, pores, grain boundaries etc., will lead to an angle deviation of the local magnetization from the easy axis. As an addition to the uniaxial anisotropy field of the film, the external field H_b will force the local magnetic moments align more closely to the easy axis. Consequently, the contribution of the spin wave states generated from the non-uniform mode and herewith the contribution of the TMS and other potential damping mechanisms to the extrinsic linewidth will be intensively suppressed by the external magnetic field [22].

In order to demonstrate respective quantitative contributions of intrinsic and extrinsic parts to the microwave damping linewidth, a FMR characterization technique is employed to investigate the dependences of the resonance field H_{RES} and linewidth ΔH_{RES} on the direction of the external static magnetic field. Fig. 6 shows the film plane and the field geometry for FMR analysis. The external field H is applied at an angle θ relative to the film normal. Because the in-plane anisotropy H_k of the sample is much less than H_{RES}, the influence of H_k to measurement results is ignored. Fig. 7 illustrates the theoretical and experimental dependences of the resonance field H_{RES} on the angle θ of the external field. It can be observed that H_{RES} is very large and reduces very fast while $\theta < 20^\circ$, which indicates that tipping magnetic moments M out of the plane needs large external field. The absence of the data at $\theta < 2^\circ$ implies that the external field is insufficient to saturate the magnetization and the saturation magnetization $4\pi M_s$ of the sample is larger than 1.4 T. While $\theta > 20^\circ$, H_{RES} reduces slowly. The dependence of H_{RES} on θ, namely H_{RES}–θ relation, was well fitted by Eq. (6) in Ref. [5], which is shown by the solid line in Fig. 7.

As mentioned in Ref. [5], the dependence of the linewidth on the external static field orientation may help clarify the two magnon contribution to the linewidth. If the angle between the external static field and the sample normal is varied, the position of the spinwave manifold is shifted relative to the FMR frequency. The number of degenerate spinwaves to which the uniform mode can couple in the two magnon process, and hence the linewidth, will change accordingly. Fig. 8 illustrates theoretical and experimental dependences of the linewidth ΔH_{RES} on angle θ. Here, it is

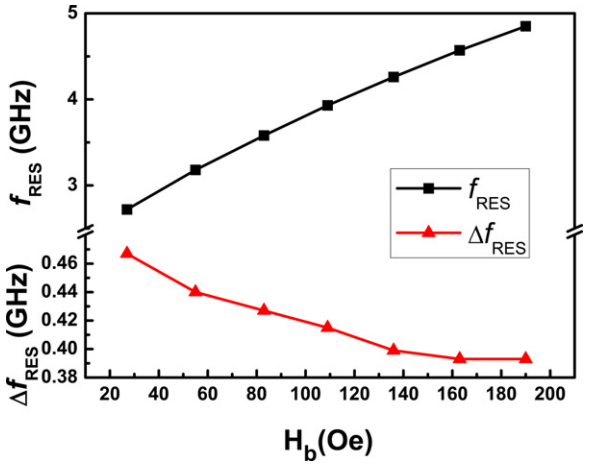

Fig. 5. The dependences of f_{RES} and Δf_{RES} on external fields H_b.

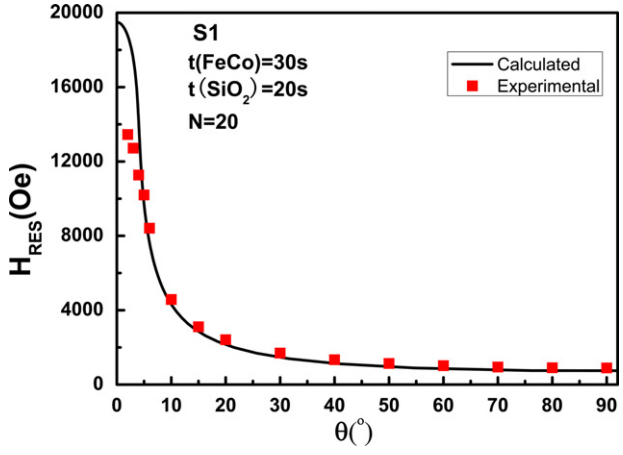

Fig. 7. The theoretical and experimental dependences of the resonance field H_{RES} on the angle θ of the external field.

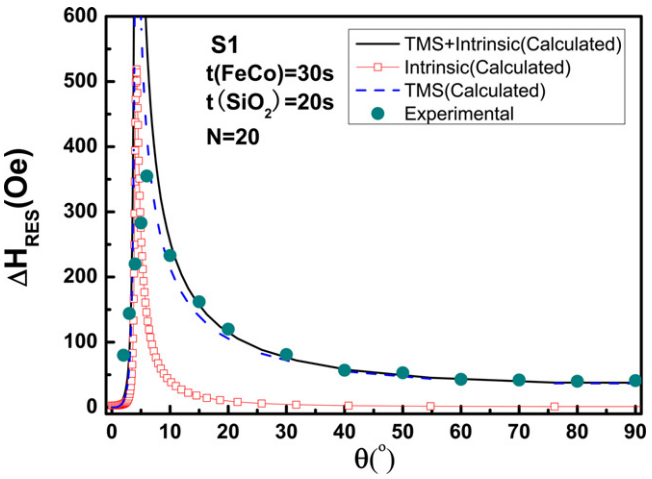

Fig. 8. The theoretical and experimental dependences of the linewidth ΔH_{RES} on angle θ of the external field (θ as shown in Fig. 6). The dark cyan dots show experimental result. The blue dashed line shows the calculated TMS result. The red line and squares show the calculated intrinsic damping result. The black line shows the sum of TMS and intrinsic damping. (For interpretation of the references to color in this figure legend, the reader is referred to the web version of the article.)

supposed that the linewidth from the extrinsic damping mainly comes from the TMS and could be calculated using a modified SLK TMS model [5]. Some internal parameters of the sample can be obtained from the fitting: ratio of the total scatterer volume to the sample volume $p = 0.0039$, scatterer radius $R = 25$ nm, L–L relaxation rate $\lambda = 55$ MHz, intrinsic frequency linewidth $\Delta\omega = 20$ MHz, $4\pi M_s = 1.96$ T. These values are all typical data for the FeCo-based ferromagnetic films and reasonable for the experimental results. In Fig. 8, while $\theta = 0^\circ$, there is essentially no TMS contribution but the L–L intrinsic damping is nonzero. As θ increases, both contributions rise up very sharply and subsequently diminish rapidly while $\theta > 4.2^\circ$. The linewidth from TMS is 1.65 times as big as the L–L damping linewidth while $\theta = 4.2^\circ$. As the external field is rotated into the film plane at $\theta = 90^\circ$, the L–L linewidth reduces to the same value as $\theta = 0^\circ$ but TMS linewidth slightly drops to a value of 36 times bigger than L–L linewidth. It is no doubt that in our multilayer sample, the TMS contribution is the most important origin of the microwave damping, which mainly comes from the imperfection in interfaces and pores in those layers.

It should be especially mentioned that the physical nature of spin transport in $[FM/NMI]_n$ multilayer films will be quite different from that in $[FM/NMM]_n$ multilayer films. According to the statement of Heinrich [12,13], in the $[FM/NMM]_n$ multilayer films, vectorial spins can transfer by the electric current flowing through the interfaces of the magnetic films and the non-magnetic metal layers. The transfer of spins will lead to an additional relaxation torque to the Gilbert intrinsic damping. But this electric current will be not excited in the $[FM/NMI]_n$ multilayer films where the non-magnetic metal layers are replaced by the insulating layers. Besides, the special structure of the $[FM/NMI]_n$ multilayer films can supply more abundant heterogeneous interfaces, and lead to more remarkable inhomogeneities of the magnetism and microstructure. This will provide an additional coupling channel between the driven FMR mode and the degenerate spin wave mode, which makes a larger extrinsic contribution to the damping linewidth. However, more theoretical researches on these topics are beyond the scope of the present investigation which just focuses on quantitative analysis of the damping origins of the $[FM/NMI]_n$ multilayer films. More details of the spin dynamics in the $[FM/NMI]_n$ multilayer films are still under investigation.

4. Conclusions

A serial of $[Fe_{65}Co_{35}/SiO_2]_n$ multilayer films with the $[FM/NMI]_n$ structure was prepared by magnetron sputtering. The results from the VSM measurements show that all of the samples possess excellent soft magnetic properties, such as tiny coercivities and certain in-plane unixial anisotropies. The permeability spectra, in a classic Lorentzian line shape, have a legible resonance peak at 2.21 GHz with a FWHM about 0.53 GHz for a typical sample S1. The main origins of the microwave damping in some typical samples were determined by FMR and microwave permeability spectra measurement. The dependence of the resonance field and linewidth on the polar angle of the external field, derived from the FMR measurement, was well fitted by a theoretical calculation. From the fitting, it can be observed that the TMS is the main relaxation mechanism in the $[Fe_{65}Co_{35}/SiO_2]_n$ multilayer film, which makes a predominant contribution to the microwave damping linewidth.

Acknowledgment

This research was supported by the National Science Foundation of China (Grant no. 11004095).

References

[1] G.Z. Chai, D.S. Xue, X.L. Fan, X.L. Li, D.W. Guo, Appl. Phys. Lett. 93 (2008) 152516.1–152516.3.
[2] M. Pasquale, F. Celegato, M. Coisson, A. Magni, S. Perero, P. Kabos, V. Teppati, S.H. Han, J. Kim, S.H. Lim, J. Appl. Phys. 99 (2006), 08M303.1–08M303.3.
[3] S.H. Ge, D.S. Yao, M. Yamaguchi, X.L. Yang, H.P. Zuo, T. Ishii, D. Zhou, F.S. Li, J. Phys. D 40 (2007) 3660–3664.
[4] K. Ikeda, K. Kobayashi, M. Fujimoto, J. Appl. Phys. 92 (2002) 5395–5400.
[5] M.J. Hurben, C.E. Patton, J. Appl. Phys. 83 (1998) 4344–4365.
[6] M.J. Hurben, D.R. Franklin, C.E. Patton, J. Appl. Phys. 81 (1997) 7458–7467.
[7] J. Lindner, I. Barsukov, C. Raeder, C. Hassel, O. Posth, R. Meckenstock, P. Landeros, D.L. Mills, Phys. Rev. B 80 (2009) 224421.1–224421.7.
[8] K. Zakeri, J. Lindner, I. Barsukov, R. Meckenstock, M. Farle, U. von Hörsten, H. Wende, W. Keune, J. Rocker, S.S. Kalarickal, K. Lenz, W. Kuch, K. Baberschke, Z. Frait, Phys. Rev. B 76 (2007) 104416.1–104416.7.
[9] K.D. Sossmeier, F. Beck, R.C. Gomes, L.F. Schelp, M. Carara, J. Phys. D 43 (2010) 055003.1–055003.5.
[10] P. Krivosik, S.S. Kalarickal, N. Mo, S. Wu, C.E. Patton, Appl. Phys. Lett. 95 (2009) 052509.1–052509.3.
[11] N. Mo, J. Hohlfeld, M. ul Islam, C.S. Brown, E. Girt, P. Krivosik, W. Tong, A. Rebei, C.E. Patton, Appl. Phys. Lett. 92 (2008) 022506.1–022506.3.
[12] R. Urban, G. Woltersdorf, B. Heinrich, Phys. Rev. Lett. 87 (2001) 217204.1–217204.4.
[13] B. Heinrich, R. Urban, G. Woltersdorf, J. Appl. Phys. 91 (2001) 7523–7525.
[14] K.M. Seemann, F. Freimuth, H. Zhang, S. Blügee, Y. Mokrousov, D.E. Brügler, C.M. Schneider, Phys. Rev. Lett. 107 (2011) 086603.1–086603.4.
[15] V. Bekker, K. Seemann, H. Leiste, J. Magn. Magn. Mater. 270 (2004) 327–332.
[16] A. Neudert, J. Mccord, R. Schäfer, L. Schultz, J. Appl. Phys. 95 (2004) 6595–6597.
[17] P. Grunberg, J. Appl. Phys. 57 (1985) 3673–3677.
[18] P. Swiatek, F. Saurenbach, Y. Pang, P. Grünberg, W. Zinn, J. Appl. Phys. 61 (1987) 3753–3755.
[19] S.S. Kalarickal, P. Krivosik, J. Das, K.S. Kim, C.E. Patton, Phys. Rev. B 77 (2008) 054427.1–054427.8.
[20] B.K. Kuanr, R.E. Camley, Z. Celinski, J. Magn. Magn. Mater. 286 (2005) 276–281.
[21] M.C. Hickey, J.S. Moodera, Phys. Rev. Lett. 102 (2009) 137601.1–137601.4.
[22] F. Xu, X. Chen, N.N. Phuoc, X.Y. Zhang, Y.G. Ma, C.K. Ong, J. Magn. Magn. Mater. 322 (2010) 3262–3265.